

ChemComm

Accepted Manuscript



This article can be cited before page numbers have been issued, to do this please use: C. Tao, B. Chen, X. Liu, L. Zhou, X. Zhu, J. Cao, Z. Gu, Z. Zhao, L. Shen and B. Z. Tang, *Chem. Commun.*, 2017, DOI: 10.1039/C7CC05031C.



This is an Accepted Manuscript, which has been through the Royal Society of Chemistry peer review process and has been accepted for publication.

Accepted Manuscripts are published online shortly after acceptance, before technical editing, formatting and proof reading. Using this free service, authors can make their results available to the community, in citable form, before we publish the edited article. We will replace this Accepted Manuscript with the edited and formatted Advance Article as soon as it is available.

You can find more information about Accepted Manuscripts in the [author guidelines](#).

Please note that technical editing may introduce minor changes to the text and/or graphics, which may alter content. The journal's standard [Terms & Conditions](#) and the ethical guidelines, outlined in our [author and reviewer resource centre](#), still apply. In no event shall the Royal Society of Chemistry be held responsible for any errors or omissions in this Accepted Manuscript or any consequences arising from the use of any information it contains.



Journal Name

COMMUNICATION

A highly luminescent entangled metal-organic framework based on pyridine-substituted tetraphenylethene for efficient pesticide detection

Received 00th January 20xx,
Accepted 00th January 20xx

DOI: 10.1039/x0xx00000x

www.rsc.org/

Chen-Lei Tao,^{†a} Bin Chen,^{†b} Xun-Gao Liu,^{*a} Li-Jiao Zhou,^a Xiao-Li Zhu,^a Jun Cao,^a Zhi-Guo Gu,^c Zujin Zhao,^{*b} Liang Shen,^a and Ben Zhong Tang^{bd}

A novel pillared-layered entangled luminescent metal-organic framework [Zn₂(bpdC)₂(BPyTPE)] (1) (BPyTPE = (*E*)-1,2-diphenyl-1,2-bis(4-(pyridin-4-yl)phenyl)ethene) has been designed and constructed. The solvent-free 1 exhibits strong blue-green emission with an excellent fluorescence quantum yield of 99% and provides a facile and reversible method to sensitively and quantitatively detect trace pesticide of 2,6-dichloro-4-nitroaniline.

Molecules with aggregation-induced emission (AIE) can fluoresce strongly in the aggregated state and have exhibited great potentials in diverse research frontiers.¹ Tetraphenylethene (TPE) is emerging as a most popular AIE luminogen because of its simple molecular structure and splendid AIE nature, which has been widely used as an important building block for numerous luminescent materials.² Recently, considerable interests are focused on using TPE derivatives decorated with coordination groups, such as carboxylate or pyridine, to construct metal-organic frameworks (MOFs).³ The incorporation of TPE units enables MOFs to emit strong fluorescence where the nonradiative decay by intramolecular motions of TPE units is restricted in rigid MOFs. The TPE-based luminescent MOFs (LMOFs) have shown great potential in an array of high-tech applications.⁴ In particular, the LMOFs are promising fluorescence sensors to detect various substances, such as volatile organic compounds, mycotoxins and nitro explosives.^{5,6} The essential sensing

signals of changes in fluorescence intensity or wavelength are closely associated with the electron transfer from LMOFs to guests or vice versa.⁷

Pesticides are widely used in agriculture, but their residues can cause serious damages to ecological safety, and result in hazardous impacts on human health and life quality through the food chain. Hence, the rapid and selective detection of pesticides has become one of the most pressing issues concerning human health and environmental protection.⁸ For example, 2,6-dichloro-4-nitroaniline (DCN) is a broad-spectrum pesticide belonging to toxicity class IV. It has been extensively employed for control of many diseases, such as wheat powdery mildew, cotton rotten bell, and fruit trees and vegetable rot. DCN degrades slowly and can persist for a long time in the environmental conditions. Currently, the common methods of DCN detection include ion mobility spectrometry, high performance liquid chromatography or other assays requiring sophisticated instruments that are expensive and complicated.⁹ To address this situation, in this contribution, we synthesize a TPE-based ligand exhibiting prominent AIE nature, and fabricate a novel pillared-layered LMOF using it as a pillar linker. The LMOF has a remarkably high fluorescence quantum yield (Φ_F) of 99%, and performs outstandingly in DCN detection with a low detection limit down to 0.13 ppm.

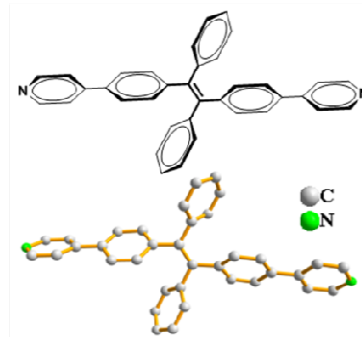


Fig. 1 Molecular and single-crystal structures of AIE-active BPyTPE.

^a College of Material, Chemistry and Chemical Engineering, Hangzhou Normal University, Hangzhou 310036, China. E-mail: xungaoliu@hznu.edu.cn

^b State Key Laboratory of Luminescent Materials and Devices, South China University of Technology, Guangzhou 510640, China. E-mail: mszjzhao@scut.edu.cn

^c School of Chemical and Material Engineering, Jiangnan University, Wuxi 214122, China

^d Department of Chemistry, Hong Kong Branch of Chinese National Engineering Research Center for Tissue Restoration and Reconstruction, The Hong Kong University of Science & Technology, Clear Water Bay, Kowloon, Hong Kong, China

†Chen-Lei Tao and Bin Chen contributed equally
*Electronic Supplementary Information (ESI) available: experimental details, crystallographic data, CIF files, thermal analysis, absorption and emission spectra, geometrical structures, PXRD patterns and fluorescence titration. See DOI: 10.1039/x0xx00000x

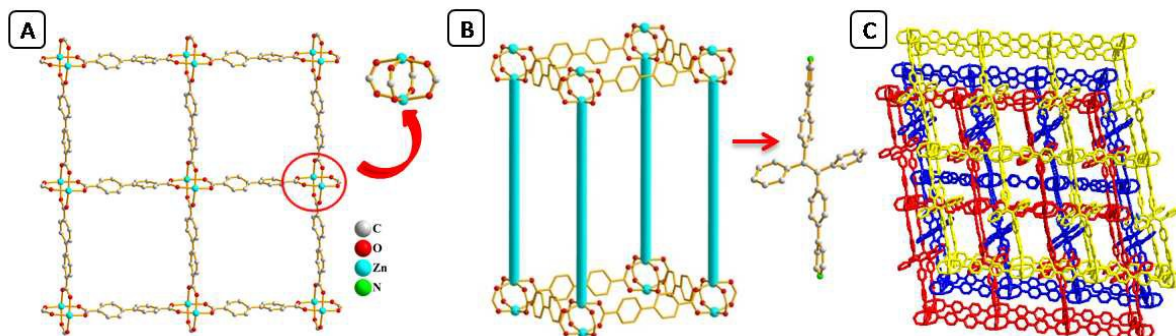


Fig. 2 (A) Topological representation of rhombic 4^4 two-dimensional paddle-wheel layer with an indicated structure of paddle-wheel SBU $[\text{Zn}_2(\text{COO})_4]$. (B) Single net of complex **1** viewed along the *a*-axis, showing pores that are closed up the interpenetration. (C) Overall crystal structure of complex **1** demonstrating the three-fold interpenetration and 1D pore running along the *b*-axis. Hydrogen atoms are omitted, and solvent molecules are removed by using the SQUEEZE routine of PLATON for clarity.

The TPE-based ligand (*E*)-1,2-diphenyl-1,2-bis(4-(pyridin-4-yl)phenyl)ethene (BPyTPE) is synthesized according to the synthetic route outlined in Scheme S1. The crude product of BPyTPE is purified by column chromatography to afford pure target compound with a *trans*-conformation, which is confirmed by the single-crystal structure (Fig. 1). The treatment of BPyTPE with $\text{Zn}(\text{NO}_3)_2 \cdot 6\text{H}_2\text{O}$ and biphenyl-4,4'-dicarboxylic acid (H_2bpdc) in a mixed solvent of *N,N*-dimethylacetamide and *N,N*-dimethylformamide yields colorless cube-like crystals of complex **1**. The complex **1** belongs to triclinic crystal system, space group *P* $\bar{1}$ (Table S1). Each Zn^{2+} ion coordinates to four carboxylate oxygen atoms from different bpdc^{2-} anions and one pyridine nitrogen atom of BPyTPE ligand, which can be seen as a tetragonal pyramid. The bond lengths of Zn-O/N are in the range of 2.000–2.038 Å, and the bond angles of O-Zn-O and O-Zn-N are approximately 86.380–89.714° and 95.406–105.058°, respectively. Two Zn^{2+} ions are bridged by four carboxylic groups to form a paddle-wheel secondary building unit (SBU) $[\text{Zn}_2(\text{COO})_4]$.^{5b} Each SBU is linked by coshared carboxylate groups of bpdc^{2-} ligands, generating a rhombic 4^4 two-dimensional (2D) network with a cross section of $22.52 \times 20.09 \text{ \AA}^2$ (Fig. 2A). Two adjacent layers are connected by BPyTPE pillar linkers with an inter-layer distance of about 21.27 Å to furnish a stable three-dimensional (3D) framework (Fig. 2B). A three-fold interpenetration is observed for the overall structure of complex **1** (Fig. 2C), and the pore volume of complex **1** is calculated to be 1793.3 \AA^3 , corresponding to a void of around 33.2% per unit cell (5403.2 \AA^3 total).¹⁰ The geometrical conformation for BPyTPE in complex **1** is further investigated (Fig. S1, ESI†). It is found that BPyTPE in complex **1** adopts a more twisted conformation with larger dihedral angles between aromatic moieties than BPyTPE in single crystals (Table S2). There are only very weak π - π stacking interactions between the phenyl rings from bpdc^{2-} ions and pyridine rings from BPyTPE ligands, with the distances of 3.540 and 3.707 Å (Fig. S2, ESI†), while no π - π stacking interactions are observed between TPE units that are mainly responsible for the light emission.

Complex **1** is stable in THF or water as indicated by powder X-ray diffraction patterns (PXRD) results (Fig. S3). It can undergo solvent exchanged with dichloromethane (DCM),

followed by drying under vacuum at room temperature to furnish solvent-free **1** sample. The result of powder X-ray diffraction patterns confirms that solvent-free **1** retains the original framework without any collapsing (Fig. S3, ESI†). Thermogravimetric analysis of complex **1** reveals 22% initial weight loss by heating from room temperature to 145 °C in N_2 stream, which is attributed to the loss of solvent molecules. A plateau appears between 145 and 405°C, followed by a sharp weight loss (~53%) corresponding to the decomposition of the framework. However, there is no obvious weight change until 405°C of solvent-free **1**, indicating the solvent molecules in complex **1** have been removed completely (Fig. S4, ESI†).

BPyTPE shows an absorption maximum at 335 nm in THF solution (Fig. S5, ESI†), associated to the π - π^* transition of the conjugated backbone. Like most TPE derivatives, BPyTPE is almost nonfluorescent in dilute THF solution because of the active intramolecular rotation. But as the aggregate formation by adding a large amount of water into the THF solution of BPyTPE, an emission peak at 502 nm enhances swiftly (Fig. 3A), which is ascribed to the restriction of intramolecular rotations and thus block of nonradiative decay of excited state. These emission behaviours demonstrate the AIE nature of BPyTPE. Solvent-free **1** exhibits strong blue-green emission at 490 nm (Fig. 3B), and complex **1** shows intense emission peaking at 498 nm, which is close to the emission of BPyTPE aggregate. The emission of solvent-free **1** is blue-shifted by 8 nm than that of complex **1**. This blue-shift phenomenon often

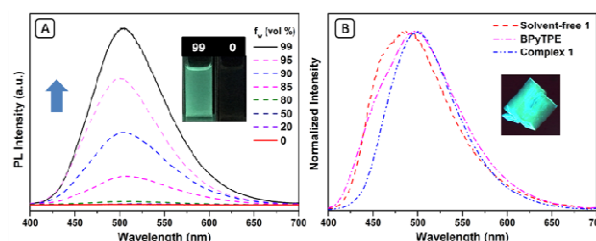


Fig. 3 (A) Photoluminescence (PL) spectra of BPyTPE in THF/water mixtures with various water fractions (f_w). Inset: photos of BPyTPE in THF/water mixtures ($f_w = 99$ and 0 vol%). (B) Solid-state PL spectra of complex **1**, solvent-free **1** and BPyTPE. Inset in B: the fluorescence photo of complex **1** ($\lambda_{\text{exc}} = 365 \text{ nm}$).

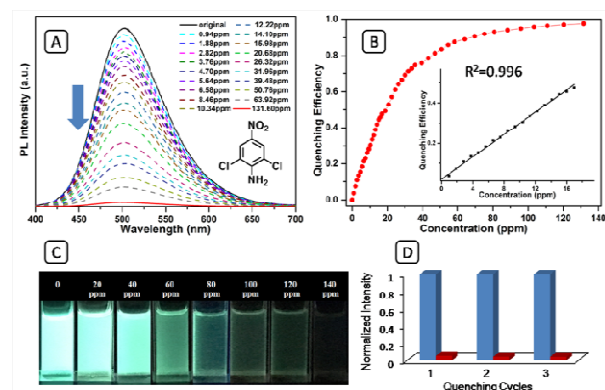


Fig. 4 (A) Fluorescence titration of solvent-free **1** in dichloromethane suspension of 2,6-dichloro-4-nitroaniline (DCN) with different concentrations ($\lambda_{\text{ex}} = 365 \text{ nm}$). (B) Correlation between the quenching efficiency and concentration of DCN. (C) Fluorescence photos of solvent-free **1** in suspensions with gradually increased DCN. (D) The result of DCN for three continuous quenching cycles. The blue bars represent the initial fluorescence intensity and the red bars represent the intensity upon addition of DCN (96 ppm).

appears in reported LMOFs, which is probably due to the decreased inter ligand coupling. Both solvent-free **1** and complex **1** have excellent Φ_{F} values of 99% and 79%, respectively, determined by a calibrated integrating sphere, thanks to the AIE nature of BPyTPE ligand. Both values are much higher than that of BPyTPE solid ($\Phi_{\text{F}} = 43\%$), owing to the greatly reduced intramolecular motion of BPyTPE when coordinated within the rigid framework. Moreover, when the turbulence of highly disordered solvent molecules is removed, the excited state energy loss is depressed to minimal, rendering a remarkably high Φ_{F} approaching to unit of solvent-free **1**. BPyTPE solid, complex **1** and solvent-free **1** exhibit fluorescence lifetimes (τ) of 3.11, 2.85 and 2.39 ns, respectively. This tendency of shorter τ and higher Φ_{F} may result from the immediate release of excited energy via fluorescence, which is the same as the findings like other TPE-based MOF PCN-94.^{3f,11}

The sensing application of solvent-free **1** in DCM suspension (0.15 mg mL^{-1} , Fig. S6 and Table S3, ESI[†]) is firstly evaluated by titration experiments with different electron rich aromatics, such as toluene, *m*-xylene, mesitylene and aniline (Fig. S7, ESI[†]). These tested samples can only slightly enhance the emission intensity. However, the emission of solvent-free **1** can be quenched by nitrobenzene, owing to the excited state electron transfer from donor (LMOFs) to acceptor (nitrobenzene guests). The quenching efficiency (QE) is estimated using the formula $(I_0 - I)/I_0$, where I_0 and I are the emission intensities of solvent-free **1** before and after adding guest molecules. As shown in Fig. S8, the emission starts to decrease upon addition of 58 ppm nitrobenzene, and is quenched greatly at a concentration of 1800 ppm with a high quenching efficiency of 98%. It is found that the detection sensitivity of nitro aniline is much higher than those of nitrobenzene and 1,2,3,4,5-pentachloro-6-nitrobenzene at the

same conditions (Fig. S9 and Fig. S14, ESI[†]). When 55 ppm *p*-nitroaniline is dispersed into the solvent-free **1** suspension, the emission is almost totally quenched (QE = 98%) (Fig. S10, ESI[†]). The detection limit is as low as $\sim 4.9 \times 10^{-2}$ ppm, calculated with $3\sigma/k$ (σ : standard deviation; k : slope).⁴ The higher selectivity of solvent-free **1** towards nitro aniline (Fig. S11, ESI[†]) probably results from hydrogen bonding interactions (N-H \cdots O) between amino of guests and oxygen of bpd²⁻.

The high sensitivities and low detection limits of solvent-free **1** towards nitro anilines inspire us to develop an assay for DCN, which has never been achieved by LMOFs previously. Fig. 4A and 4B show the spectra of decline in emission intensity and the linear quenching range of solvent-free **1** upon the addition of DCN (Fig. S12, ESI[†]). The strong emission of solvent-free **1** is quenched drastically, which can be observed by naked eye (Fig. 4C). A quantitative detection of DCN ranged from 0.94 to 16.92 ppm is established with a low detection limit of 0.13 ppm. To confirm the limit of detection, the fluorescence titration of DCN at low concentrations from 0.13 ppm to 0.80 ppm is further performed, and a linear proportion of I_0/I is obtained (Fig. S13, ESI[†]). Solvent-free **1** can be reused after centrifuging the suspension and washing with DCM by several times (Fig. 4D), without degradation in detection performance. According to China National food safety standard-Maximum residue limits for pesticides in food, the maximum residue limits for DCN is 7 ppm in fruits of nectarine and grapes, and 15 ppm in vegetables of carrots.¹² Obviously, solvent-free **1** can perform outstandingly in detection of the fruit fungicide of DCN and is competent to fulfill the requirements. To deepen insight into the mechanism for detecting DCN, the HOMO and LUMO energy levels of DCN and BPyTPE in complex **1** are calculated (Fig. S15, ESI[†]). The excited state electron transfer from the higher LUMO of BPyTPE (-1.77 eV) to that of DCN (-2.40 eV) may occur, resulting in severe fluorescence quenching. Therefore, the photoinduced electron-transfer (PET)¹³ may be the sensing mechanism. Furthermore, hydrogen bonding interactions between complex **1** and DCN should also contribute to the good sensitivity of the detection.

In summary, we have synthesized a TPE-based ligand (BPyTPE) with a *trans*-conformation and prominent AIE property. Based on BPyTPE, we have developed a novel pillared-layered LMOF (complex **1**) with a three-fold interpenetration structure. Solvent-free **1** exhibits intense blue-green emission at 498 nm with a remarkably high Φ_{F} of 99%. The emission of solvent-free **1** can be quenched efficiently and selectively by nitro aniline. Based on solvent-free **1**, we establish a reversible method to sensitively and quantitatively detect trace pesticide DCN, with a linear range of 0.94–16.92 ppm and a low detection limit of 0.13 ppm. To the best of our knowledge, using LMOF as a fluorescent sensor to efficiently detect DCN is very rare and the present assay method is a promising one capable of practical application. Further studies of detecting other pesticides as well as heavy metal pollutants with TPE-based LMOFs are in progress.

We thank the financial support from the National Natural Science Foundation of China (21671051 and 21673082), the

Zhejiang Provincial Natural Science Foundation of China (LY15B010006, LY16B010003) and the Innovative Research Team in Chinese University (IRT 1231). Z.Z. thanks the financial support from Guangdong Natural Science Funds for Distinguished Young Scholar (2014A030306035). We also thank Dr Zaichao Zhang for his assistance in crystallographic analysis.

Notes and references

- (a) J. Mei, Y. Hong, J. W. Y. Lam, A. Qin, Y. Tang and B. Z. Tang, *Adv. Mater.*, 2014, **26**, 5429; (b) J. Mei, N. L. C. Leung, R. T. K. Kwok, J. W. Y. Lam and B. Z. Tang, *Chem. Rev.*, 2015, **115**, 11718; (c) Y. Hong, J. W. Y. Lam and B. Z. Tang, *Chem. Soc. Rev.*, 2011, **40**, 5361.
- (a) X. Yan, T. R. Cook, P. Wang, F. Huang and P. J. Stang, *Nat. Chem.*, 2015, **7**, 342; (b) C. S. Diercks and O. M. Yaghi, *Science*, 2017, **335**, 923; (c) R. Hu, N. L. C. Leung and B. Z. Tang, *Chem. Soc. Rev.*, 2014, **43**, 4494; (d) Z. Zhao, J. W. Y. Lam and B. Z. Tang, *J. Mater. Chem.*, 2012, **22**, 23726; (e) S. Dalapati, C. Gu and D. Jiang, *Small*, 2016, **47**, 6513–6527.
- (a) Y. Cui, B. Li, H. He, W. Zhou, B. Chen and G. Qian, *Acc. Chem. Res.*, 2016, **49**, 483; (b) N. B. Shustova, A. F. Cozzolino and M. Dincă, *J. Am. Chem. Soc.*, 2012, **134**, 19596; (c) N. B. Shustova, T.-C. Ong, A. F. Cozzolino, V. K. Michaelis, R. G. Griffin and M. Dincă, *J. Am. Chem. Soc.*, 2012, **134**, 15061; (d) Q. Gong, Z. Hu, B. J. Deibert, T. J. Emge, S. J. Teat, D. Banerjee, B. Mussman, N. D. Rudd and J. Li, *J. Am. Chem. Soc.*, 2014, **136**, 16724; (e) Z. Zhou, C. He, J. Xiu, L. Yang and C. Duan, *J. Am. Chem. Soc.*, 2015, **137**, 15066; (f) Z. Wei, Z.-Y. Gu, R. K. Arvapally, Y.-P. Chen, R. N. McDougald, J. F. Ivy, A. A. Yakovenko, D. Feng, M. A. Omary and H.-C. Zhou, *J. Am. Chem. Soc.*, 2014, **136**, 8269; (g) M. Zhang, G. Feng, Z. Song, Y.-P. Zhou, H.-Y. Chao, D. Yuan, T. T. Y. Tan, Z. Guo, Z. Hu, B. Z. Tang, B. Liu and D. Zhao, *J. Am. Chem. Soc.*, 2014, **136**, 7241; (h) Y. Wang, B. Yuan, Y.-Y. Xu, X.-G. Wang, B. Ding and X.-J. Zhao, *Chem. Eur. J.*, 2015, **21**, 2107.
- (a) V. W.-W. Yam, V. K.-M. Au and S. Y.-L. Leung, *Chem. Rev.*, 2015, **115**, 7589; (b) Z. Hu, W. P. Lustig, J. Zhang, C. Zheng, H. Wang, S. J. Teat, Q. Gong, N. D. Rudd and J. Li, *J. Am. Chem. Soc.*, 2015, **137**, 16209; (c) X.-G. Liu, H. Wang, B. Chen, Y. Zou, Z.-G. Gu, Z. Zhao and L. Shen, *Chem. Commun.*, 2015, **51**, 1677; (d) Q. Zhang, J. Su, D. Feng, Z. Wei, X. Zou and H.-C. Zhou, *J. Am. Chem. Soc.*, 2015, **137**, 10064; (e) A. Douvali, A. C. Tsipis, S. V. Eliseeva, S. Petoud, G. S. Papaefstathiou, C. D. Malliakas, I. Papadas, G. S. Armatas, I. Margiolaki, M. G. Kanatzidis, T. Lazarides and M. J. Manos, *Angew. Chem., Int. Ed.*, 2015, **54**, 1651.
- (a) Y. Cui, Y. Yue, G. Qian and B. Chen, *Chem. Rev.*, 2012, **112**, 1126; (b) Y. Takashima, V. M. Martínez, S. Furukawa, M. Kondo, S. Shimomura, H. Uehara, M. Nakahama, K. Sugimoto and S. Kitagawa, *Nat. Commun.*, 2011, **2**, 168; (c) X. He and V. W.-W. Yam, *Coordin. Chem. Rev.*, 2011, **255**, 2111; (d) L. Wang, G. Fan, X. Xu, D. Chen, L. Wang, W. Wang and P. Cheng, *J. Mater. Chem. A*, 2017, **5**, 5541; (e) M.-J. Dong, M. Zhao, S. Ou, C. Zou and C.-D. Wu, *Angew. Chem., Int. Ed.*, 2014, **53**, 1575; (f) Y. Guo, X. Feng, T. Han, S. Wang, Z. Lin, Y. Dong and B. Wang, *J. Am. Chem. Soc.*, 2014, **136**, 15485; (g) K. Asha, R. Bhattacharjee and S. Mandal, *Angew. Chem. Int. Ed.*, 2016, **55**, 11528; (h) Z. Chang, D.-H. Yang, J. Xu, T.-L. Hu and X.-H. Bu, *Adv. Mater.*, 2015, **27**, 5432; (i) D. Sun, S. Yuan, H. Wang, H.-F. Lu, S.-Y. Feng and D.-F. Sun, *Chem. Commun.*, 2013, **49**, 6152; (j) S. Yuan, Y.-K. Deng and D. Sun, *Chem. Eur. J.*, 2014, **20**, 10093; (k) Z.-H. Yan, X.-Y. Li, L.-W. Liu, S.-Q. Yu, X.-P. Wang and D. Sun, *Inorg. Chem.*, 2016, **55**, 1096.
- (a) L. E. Kreno, K. Leong, O. K. Farha, M. Allendorf, R. P. V. Duyne and J. T. Hupp, *Chem. Rev.*, 2012, **112**, 1105; (b) Z. Hu, B. J. Deibert and J. Li, *Chem. Soc. Rev.*, 2014, **43**, 5815; (c) X. Wang, O. S. Wolfbeis and R. J. Meier, *Chem. Soc. Rev.*, 2013, **42**, 7834; (d) X.-Z. Song, S.-Y. Song, S.-N. Zhao, Z.-M. Hao, M. Zhu, X. Meng, L.-L. Wu and H.-J. Zhang, *Adv. Funct. Mater.*, 2014, **24**, 4034; (e) S.-Y. Zhang, W. Shi, P. Cheng and M. J. Zaworotko, *J. Am. Chem. Soc.*, 2015, **137**, 12203; (f) B. Z.-Z. Lu, R. Zhang, Y.-Z. Li, Z.-J. Guo and H.-G. Zheng, *J. Am. Chem. Soc.*, 2011, **133**, 4172; (g) X.-L. Hu, F.-H. Liu, H.-N. Wang, C. Qin, C.-Y. Sun, Z.-M. Su and F.-C. Liu, *J. Mater. Chem. A*, 2014, **2**, 14827.
- (a) Y. Li, S.-S. Zhang and D.-T. Song, *Angew. Chem. Int. Ed.*, 2013, **52**, 710; (b) M. D. Allendorf, C. A. Bauer, R. K. Bhakta and R. J. T. Houk, *Chem. Soc. Rev.*, 2009, **38**, 1330; (c) C. A. Kent, D.-M. Liu, T. J. Meyer and W. Lin, *J. Am. Chem. Soc.*, 2012, **134**, 3991; (d) L.-Y. Guo, H.-F. Su, M. Kurmoo, X.-P. Wang, Q.-Q. Zhao, S.-C. Lin, C.-H. Tung, D. Sun and L.-S. Zheng, *ACS Appl. Mater. Interfaces.*, 2017, **9**, 19980; (e) W.-M. Chen, X.-L. Mneg, G.-L. Zhuang, Z. Wang, M. Kurmoo, Q.-Q. Zhao, X.-P. Wang, B. Shan, C.-H. Tung and D. Sun, *J. Mater. Chem. A*, 2017, **5**, 13079; (f) X.-G. Hou, Y. Wu, H.-T. Cao, H.-Z. Sun, H.-B. Li, G.-G. Shan and Z.-M. Su, *Chem. Commun.*, 2014, **50**, 6031; (g) G.-G. Shan, H.-B. Li, H.-Z. Sun, D.-X. Zhu, H.-T. Cao and Z.-M. Su, *J. Mater. Chem. C*, 2013, **1**, 1440.
- (a) M. R. Azhara, H. R. Abid, H. Sun, V. Periasamy, M. O. Tade and S. Wang, *J. Colloid Interface Sci.*, 2016, **478**, 344; (b) H. Su, Y. Lin, Z. Wanga, Y.-L. E. Wong, X. Chen and T.-W. D. Chan, *J. Chromatogr. A*, 2016, **1466**, 21; (c) S. Li, X. Zhang and Y. Huang, *J. Hazard. Mater.*, 2017, **321**, 711.
- (a) Y. Yao, Y. Wena, L. Zhang, Z. Wang, H. Zhang and J. Xu, *Anal. Chim. Acta.*, 2014, **831**, 38; (b) S. Mosleh and M. R. Rahimi, *Ultrason. Sonochem.*, 2017, **35**, 449; (c) C. Guo, Q. Jin, Y. Wang, B. Ding, Y. Li, J. Huo and X. Zhao, *Sens. Actuators, B*, 2016, **234**, 184.
- Spek, A. L. PLATON: A Multipurpose Crystallographic Tool; Utrecht University: Utrecht, The Netherlands, 2001.
- Y. Fushimi, M. Koinuma, Y. Yasuda, K. Nomura and M. S. Asano, *Macromolecules*, 2017, **50**, 1803.
- National food safety standard—Maximum residue limits for pesticides in food. ICS 65.100. GB 2763–2014.
- (a) Y. Zhao, X. Xu, L. Qiu, X. Kang, L. Wen and B. Zhang, *ACS Appl. Mater. Interfaces*, 2017, **9**, 15164; (b) S. S. Nagarkar, A. V. Desai and S. K. Ghosh, *Chem. Commun.*, 2014, **50**, 8915; (c) M. Gao, Y. Wu, B. Chen, B. He, H. Nie, T. Li, F. Wu, W. Zhou, J. Zhou and Z. Zhao, *Polym. Chem.*, 2015, **6**, 7641.